Single Polymer-Based Ternary Electronic Memory Material and Device

Shu-Juan Liu, Peng Wang, Qiang Zhao, Hui-Ying Yang, JenIt Wong, Hui-Bin Sun, Xiao-Chen Dong,* Wen-Peng Lin, and Wei Huang**

The exponential growth of information communication and the miniaturization of electronic devices have paved the way for the development of a new strategy on memory materials and devices.[1,2] As a promising alternative to conventional inorganic semiconductor-based memory, organic/polymer memories have been extensively investigated for their potential as a high-density memory in three-dimensional arrays and as materials for fabricating flexible devices.[3–21] Nowadays, manufacturing organic/polymer memory devices is limited to binary materials based on electrical bistability (i.e., "0" and "1") in response to an applied electric field. Increasing the number of memory states to multilevel states and producing high-density and efficient memory devices are highly desirable.[22] However, this particular kind of device has not been fully explored due to the lack of appropriate design principles. Pal et al. demonstrated conductance switching between multilevel states based on the blend of a small molecule (Rose Bengal) and a polymer.[23] Most recently, Lu et al. developed a ternary memory device using a small organic molecule as the active material.[24] Compared with the small-molecule and blend systems, the single polymer exhibits several advantages for its application in devices, including flexibility, low cost and solution processability.[7] However, single polymer-based ternary memory materials and devices have not yet been studied.

Several kinds of switching mechanisms have been proposed on the electrical bistability of polymer memory materials, including nanocomposite redox, charge transfer (CT), conformational change, and trapping-detrapping.[25–28] Currently, we are very interested in investigating the possibility of rationally creating a ternary polymer memory device by combining two switching mechanisms in one polymer system to form two conducting channels. In this present work, we designed and synthesized a non-conjugated polymer **iamP6** with on-chain Ir(III) complexes (**Figure 1**A). Polymer **iamP6** comprises flexible spacers (O=C–O–C–C unit) for bridging the electroactive pendant chromophore carbazoles (Cz) to permit a conformational change under the electric field[29] and a donor-acceptor (D-A) system containing Cz (a well-known donor) and Ir(III) complex (acceptor) to permit CT.[19,30–33] We successfully generated a prototype of a ternary memory device with **iamP6** as the active material, which could be assigned to both the conformation-induced conductance switching of Cz moieties (as the conducting channel I) and the subsequent CT from the ordered Cz to Ir(III) complex (as the conducting channel II). The resulting ternary memory performances can potentially increase the memory capacity of the device from 2^n to 3^n.

Ir(III) complex monomer **M1** containing a polymerizable double bond was synthesized using 3-bromo-propene and Ir(III) complex with 3-hydroxypicolinic acid as an ancillary ligand in the presence of K_2CO_3 in *N,N'*-dimethylformamide (DMF) (Scheme S1 in Supporting Information). The reaction of 9*H*-carbazole with 2-chloroethanol in the presence of potassium hydroxide and DMF yields 2-(9*H*-carbazol-9-yl)ethanol, which was used in synthesizing the monomer of 2-(9*H*-carbazol-9-yl) ethyl methacrylate by reacting with methacryloyl chloride in the presence of triethylamine and dry tetrahydrofuran (THF). The polymerization of Ir(III) complex and carbazole monomers was carried out with 2,2'-azobisisobutyronitrile (AIBN) as initiator at 70 °C in THF under an argon atmosphere for 12 h (Scheme S2 in Supporting Information). The resulting polymer **iamP6** was characterized by NMR and gel permeation chromatography (GPC) analysis. Based on the ^{1}H NMR data, the Ir(III) complex content in the copolymer was estimated to be 10.7%, a percentage lower than that in the feed ratio, which may be attributed to the difference in the reaction activity and/or steric hindrance of the complex unit. Polymer **iamP6** shows a weight-average molecular weight of approximately 21500 and a polydispersity index of approximately 1.33, as revealed by GPC measurement. In addition, **iamP6** exhibits good thermal stability with 5% weight-loss temperature of approximately 250 °C (Figure S1). Polymer **iamP6** can be spin-coated to form thin films with good quality. The atomic force microscopy (AFM) image shows that the film is smooth without any aggregation (Figure 1B).

Figure 1C illustrates our prototype memory device, which is similar to most reported devices with a sandwich structure comprising a layer of **iamP6** film and a pair of electrodes, indium

Prof. S. J. Liu, P. Wang, Prof. Q. Zhao, H.-B. Sun, W.-P. Lin, Prof. W. Huang
Key Laboratory for Organic Electronics & Information Displays (KLOEID)
Nanjing University of Posts & Telecommunications (NUPT)
Nanjing 210046, PR China
E-mail: iamqzhao@njupt.edu.cn; wei-huang@njupt.edu.cn
Prof. X.-C. Dong
Institute of Advanced Materials (IAM)
Nanjing University of Posts & Telecommunications (NUPT)
Nanjing 210046, PR China
E-mail: iamxcdong@njupt.edu.cn
Dr. H.-Y. Yang, J. Wong
Pillar of Engineering Product Development
Singapore University of Technology and Design
287 Ghim Moh Road, 279623, Singapore

DOI: 10.1002/adma.201104307

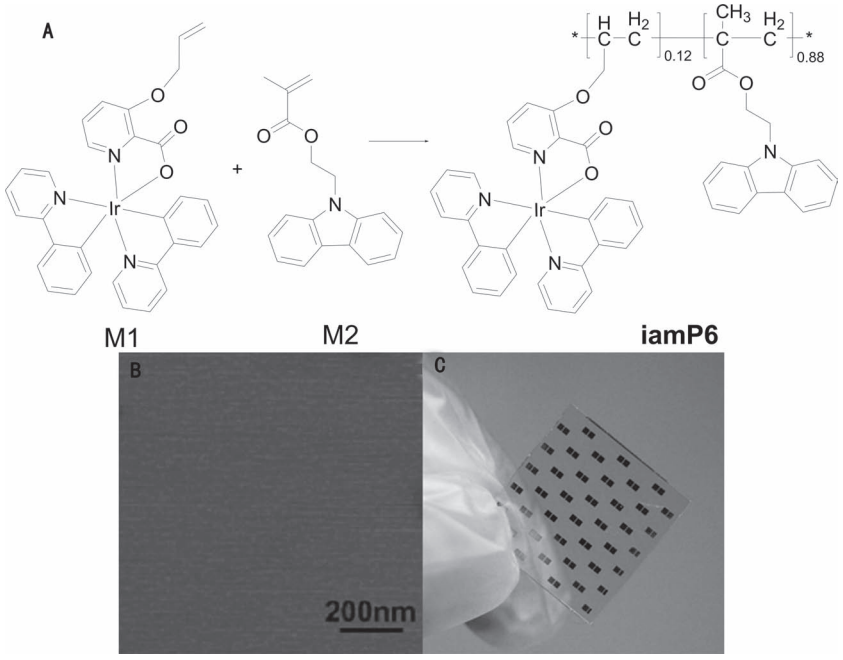

Figure 1. (A) Synthesis of iamP6, (B) AFM image of a film of iamP6, and (C) prototype memory devices.

tin oxide (ITO) and Al, as shown in **Figure 2**A.[18,19,29] Polymer **iamP6** molecule was spin-coated onto the ITO substrate with polymer film thickness of approximately 50 nm. Then, a 300 nm thick Al was deposited onto the polymer surface using a shadow mask to form the top electrode. The top Al and bottom ITO electrodes were connected to a source with varying voltages. The current that passed through the electrodes was monitored. Figure 2B shows the current-voltage (*I–V*) performances of the as-fabricated device. The first sweep of the as-fabricated device exhibited two abrupt increases in the current at the switching threshold voltages, namely –0.55 and –1.15 V, respectively (Figure 2B). This result differs from common binary memory devices with one switch in the current at threshold voltage.[7] This process demonstrates the transition from a low-conductivity state (~10^{-6} A, "0" state) to an intermediate-conductivity state (~$10^{-4.5}$ A, "1" state), and finally to a high-conductivity state (~$10^{-1.5}$ A, "2" state). The three states exhibited a distinct current ratio of $1:10^{1.5}:10^{4.5}$ for "0", "1", and "2" states. Thus, a ternary memory device was achieved.[24] These transitions from "0" to "1", and then to "2" states are similar to the "writing" process in the digital memory cell.[18,19] The low operating voltage is desirable for low-power memory devices.[7] The device remained relatively stable in the high-conductivity state ("2" state) during the subsequent negative sweep (sweep 2), indicating the nonvolatile nature of the memory effect.[18,19,21] By an inverse sweep from 0 V to 3 V (sweep 3), a switch from high-conductivity state ("2" state) to low-conductivity state ("0" state) with switching threshold voltage of 2.5 V was observed. However, the device remained in its low-conductivity state during the subsequent positive sweep from 0 V to 3 V (sweep 4). The three conductivity states were observed during the negative sweep. The conductance switching at a suitable negative voltage was associated with the memory effects in the as-fabricated device. Bias is not required to sustain the high-conductivity state. However, only a suitable positive bias can switch the high-conductivity state to a low one. This feature allows the application of **iamP6** in a ternary rewritable memory device, which exhibits flash memory behaviors.[19,21]

The electrochemical characteristics of **iamP6** were investigated using cyclic voltammetry (CV). CV was performed on the **iamP6** film coated on a working electrode in a solution of 0.10 M tetrabutylammonium hexafluorophosphate in acetonitrile at a scan rate of 100 mV/s at room temperature in a typical three-electrode cell with a working electrode (glassy carbon electrode), a reference electrode (Ag/Ag^+, referenced against ferrocene/ferrocenium (FOC)), and a counter electrode (Pt wire) in nitrogen atmosphere. The polymer **iamP6** exhibited two reversible oxidation behaviors during the scan (Figure S2). The first oxidation peak appeared at approximately 0.87 V with the onset potential at around 0.56 V. Accordingly,

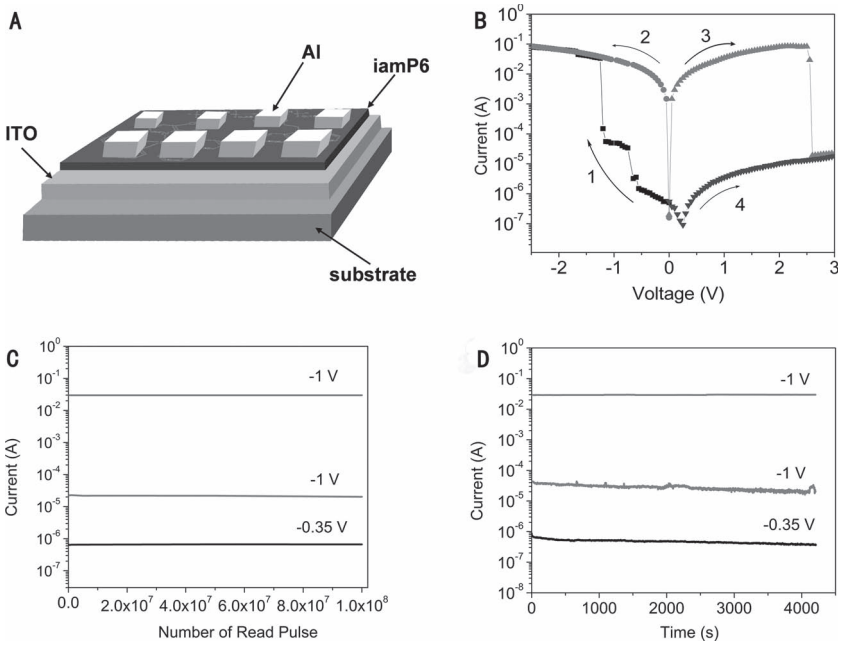

Figure 2. (A) Memory device structure based on iamP6 (ITO/iamP6/Al). (B) Typical *I–V* characteristics of an ITO/iamP6/Al device. (C) Effects of read cycles on the "0", "1" and "2" states. (D) Stability of the ITO/iamP6/Al device in "0", "1" and "2" states under a constant stress (-1.0 V for "1" and "2" states, -0.35 V for "0" state).

HOMO energy level was estimated at approximately –5.34 eV according to a previous report.[18] LUMO energy level of approximately –2.86 eV was estimated based on the HOMO level and UV-vis absorption spectrum as shown in Figure S3.[18] Thus, the energy barrier between the LUMO of **iamP6** and the work function of Al was 1.24 eV, whereas the energy barrier between the HOMO level of **iamP6** and the work function of the ITO was only 0.54 eV. These results indicate that the hole injection from the ITO into the HOMO level of **iamP6** is a favored process and **iamP6** is a *p*-type material with holes dominating the conducting process.[18,19]

Several researchers have observed and demonstrated the electrical bistability of some non-conjugated polymers with pendant active groups, such as carbazole moieties, using the mechanism of the electric-field-induced conformational change.[9,29,34–36] For example, Kang and Zhu et al. reported that poly-(2-(*N*-carbazolyl)ethyl methacrylate) and poly(2-(9*H*-carbazol-9-yl)ethyl methacrylate) exhibit write-once read-many-times (WORM) memory behaviors.[29,34] In addition, they investigated the memory mechanism in detail and demonstrated that the field-induced transition of the pendant carbazole groups from the disoriented state to the ordered face-to-face conformation is responsible for the memory behaviors. Similarly, the degree of regioregularity of polymer **iamP6** film would be low at the ground state promoted by the flexible molecular spacer between the carbazole group and the polymer backbone, which does not favor the interaction of carbazole groups.[29,34] The calculated regiorandom structure using theoretical calculations (**Figure 3**A) and X-ray diffraction (XRD) analysis (Figure S6A) further demonstrate the low degree of regioregularity of polymer **iamP6** film. As a result, the charge carriers (holes) experience difficulty in hopping through the neighboring carbazole groups because of the absence of face-to-face conformations and the presence of a lengthy distance between the neighboring carbazole groups.[29,34] Therefore, the current of the device based on **iamP6** is low and the device is in its low-conductivity state ("0" state) at low voltage (Figure 3B).

With the increase in bias on the negative scan, the hole injection from ITO causes the carbazole groups near the ITO region to be oxidized first, forming positive species,[29] because the content of carbazole groups is significantly higher than that of Ir(III) complexes. The first oxidation of carbazole groups instead of Ir(III) complex moieties is further demonstrated by the lower oxidation potential of poly(2-(9*H*-carbazol-9-yl)ethyl methacrylate) than that of the Ir(III) complex moiety (Figures S4 and S5). Thus, the charged carbazole group driven by the applied field has the tendency to attract nearby neutral carbazole groups to form a partial or complete face-to-face conformation.[29] Then, the positive charge is delocalized to the neighboring carbazole groups through more ordered conformation (Figure 3B). As the delocalization process extends with the increase in the electric field up to the required threshold value (–0.55 V), the carbazole groups in the bulk material re-organize from a regiorandom to a regioregular structure, in the general direction of the electric field toward the Al cathode. Thus, a free channel for the charge transport and a partially conductive thin film were formed.[29] The oxidized carbazole groups are further stabilized by the neighboring electron-withdrawing –O–C=O groups.[34] Thus, the formation of the intermediate-conductivity state ("1" state) occurred and reached stability between –0.55 V and –1.15 V (Figure 3B). The field-induced conformational change was also investigated by comparing the XRD spectra of **iamP6** film obtained before and after applying negative voltage (Figures S6A and S6B). The XRD results show that the diffraction peak centered at $2\theta = 8.7°$ became evidently sharper and stronger after applying negative voltage, indicating that the degree of regioregularity of polymer **iamP6** film increased significantly due to the voltage-induced conformation ordering in the polymer film. The CT process can occur as the sweep from –1.15 V to –3.0 V continues, with the charges transferring from the ordered carbazole moieties to Ir(III) complex moieties to form the CT state.[19] Consequently, another charge-transporting channel was formed, resulting in a high-conductivity state ("2" state). Therefore, two free charge-transporting channels can be generated from **iamP6**, and a ternary memory device is produced successfully by combining both the conformational change and the CT mechanisms. However, only one switch from the high-conductivity state to the low-conductivity state at the switching threshold voltage of 2.5 V was observed during the inverse sweep. It is well known that the formed CT complex can decompose under a reverse bias.[25,33] In addition, the transformation from a regioregular arrangement to a regiorandom one, via the field-induced conformation change, was demonstrated by the change of XRD spectrum (Figure S6C) of **iamP6** film obtained after applying a negative and subsequently a positive voltage, and the diffraction peak centered at $2\theta = 8.7°$ became weaker evidently when compared with that in Figure S6B, which indicates the decrease of the regioregularity degree of polymer film. Hence, a reverse bias is likely to dissociate the CT complex and break the regioregular carbazole moieties. Thus, the device returns to low-conductivity (Figure 3B).

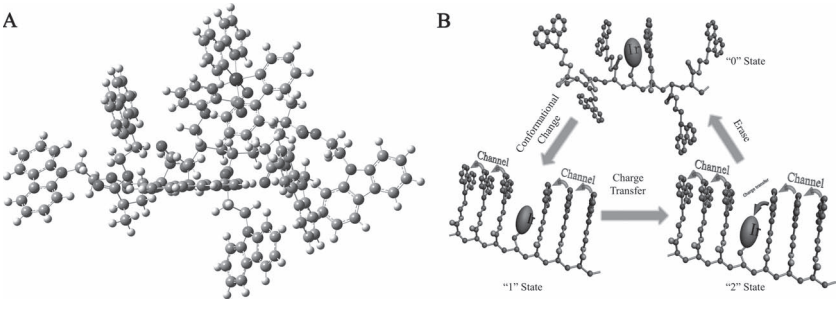

Figure 3. (A) Optimized geometry of iamP6 and (B) the proposed memory mechanism.

The parameters of the as-fabricated memory device were evaluated under ambient conditions. The effect of continuous read pulses of –0.35 V on the "0" state and –1.0 V on the "1" and "2" states was investigated. As shown in Figure 2C, no evident degradation in the current was observed in these three states after more than 100 million (10^8) read cycles. This finding demonstrates their excellent retention. The stability of the device under a constant stress of –0.35 V or –1.0 V is shown in Figure 2D. Any evident degradation in the current of the "0", "1", and "2" states

was not observed during the test. These results demonstrate the excellent memory effects of polymer **iamP6**.

In summary, we have presented the first ternary memory device based on a single polymer with on-chain Ir(III) complexes by combining both the conformational change and CT mechanisms. We have also successfully demonstrated excellent ternary memory performances, including low reading, writing and erasing voltages, and good stability for the three states. Although the detailed mechanism for the ternary memory behaviors need to be further clarified through experimental and theoretical methods, as a proof-of-concept, we hope that the proposed principle combining the multiple memory mechanisms in one polymer system would open up a new and efficient avenue for the design of high-density polymer memory materials and devices. We are now actively pursuing more polymer-based ternary memory materials and devices based on our design principle.

Experimental Section

Fabrication and Characterization of the Memory Device: The indium-tin-oxide glass substrate was precleaned with water, acetone, and then 2-propanol in an ultrasonic bath (15 min each). A toluene solution of **iamP6** (10 mg mL^{-1}) was spin-coated onto ITO substrate, followed by solvent removal in a vacuum chamber at 10^{-5} Torr and 50 °C. The thickness of the polymer layer was about 50 nm. A 390-nm-thick aluminum top electrode was thermally evaporated onto the polymer surface at a pressure around 10^{-7} Torr. The measurements were carried out on devices of 0.4 × 0.4 mm^2 in size. The devices were characterized under ambient conditions, using a Hewlett–Packard 4156A semiconductor parameter analyzer equipped with an Agilent 16440A SMU/pulse generator.

Theoretical Calculations: All calculations were carried out with the Gaussian 03 package.[37] The optimization of the complex structure was performed using B3LYP density functional theory. The LANL2DZ basis set was used to treat the Ir atom. For all other atoms, the 6-31G basis set was used.

Supporting Information

Supporting Information is available from the Wiley Online Library or from the author.

Acknowledgements

This work was financially supported by the National Natural Science Foundation of China (21174064, 21171098 and 61076067), National Basic Research Program of China (973 Program, 2009CB930601 and 2012CB933300), Natural Science Fund for Colleges and Universities in Jiangsu Province (10KJB430010), the Ministry of Education of China (No. IRT1148), A Project Funded by the Priority Academic Program Development of Jiangsu Higher Education Institutions, and Nanjing University of Posts and Telecommunications (NY210029 and NY211003). H. Y. Yang would like to thank SUTD international design center for funding support.

Received: November 10, 2011
Revised: February 3, 2012
Published online: April 27, 2012

[1] J. C. Scott, L. D. Bozano, *Adv. Mater.* **2007**, *19*, 1452.
[2] S. Moller, C. Perlov, W. Jackson, C. Taussig, S. R. Forrest, *Nature* **2003**, *426*, 166.
[3] R. G. Hicks, *Nat. Chem.* **2011**, *3*, 189.
[4] Y. K. Fang, C. L. Liu, G. Y. Yang, P. C. Chen, W. C. Chen, *Macromolecules* **2011**, *44*, 2604.
[5] Y. K. Fang, C. L. Liu, C. Li, C. J. Lin, R. Mezzenga, W. C. Chen, *Adv. Funct. Mater.* **2010**, *20*, 3012.
[6] A. Bandyopadhyay, S. Sahu, M. Higuchi, *J. Am. Chem. Soc.* **2011**, *133*, 1168.
[7] Q. D. Ling, D. J. Liaw, C. X. Zhu, D. S. H. Chan, E. T. Kang, K. G. Neoh, *Prog. Polym. Sci.* **2008**, *33*, 917.
[8] K. L. Wang, Y. L. Liu, J. W. Lee, K. G. Neoh, E. T. Kang, *Macromolecules* **2010**, *43*, 7159.
[9] H. Li, N. J. Li, R. Sun, H. W. Gu, J. F. Ge, J. M. Lu, Q. F. Xu, X. W. Xia, L. H. Wang, *J. Phys. Chem. C* **2011**, *115*, 8288.
[10] E. Kapetanakis, A. M. Douvas, D. Velessiotis, E. Makarona, P. Argitis, N. Glezos, P. Normand, *Adv. Mater.* **2008**, *20*, 4568.
[11] Y. Yang, J. Y. Ouyang, L. P. Ma, R. J. Tseng, C. W. Chu, *Adv. Funct. Mater.* **2006**, *16*, 1001.
[12] R. C. G. Naber, K. Asadi, P. W. M. Blom, D. M. de Leeuw, B. de Boer, *Adv. Mater.* **2010**, *22*, 933.
[13] A. Bandyopadhyay, A. J. Pal, *Adv. Mater.* **2003**, *15*, 1949.
[14] C. W. Chu, J. Ouyang, J. H. Tseng, Y. Yang, *Adv. Mater.* **2005**, *17*, 1440.
[15] N. H. You, C. C. Chueh, C. L. Liu, M. Ueda, W. C. Chen, *Macromolecules* **2009**, *42*, 4456.
[16] T. W. Kim, H. Choi, S. H. Oh, G. Wang, D. Y. Kim, H. Hwang, T. Lee, *Adv. Mater.* **2009**, *21*, 2497.
[17] S. Park, T. J. Lee, D. M. Kim, J. C. Kim, K. Kim, W. Kwon, Y. G. Ko, H. Choi, T. Chang, M. Ree, *J. Phys. Chem. B* **2010**, *114*, 10294.
[18] Q. D. Ling, Y. Song, E. Y. H. Teo, S. L. Lim, C. X. Zhu, D. S. H. Chan, D. L. Kwong, E. T. Kang, K. G. Neoh, *Electrochem. Solid-State Lett.* **2006**, *9*, G268.
[19] S. J. Liu, Z. H. Lin, Q. Zhao, Y. Ma, H. F. Shi, M. D. Yi, Q. D. Ling, Q. L. Fan, C. X. Zhu, E. T. Kang, W. Huang, *Adv. Funct. Mater.* **2011**, *21*, 979.
[20] T. L. Choi, K. H. Lee, W. J. Joo, S. Lee, T. W. Lee, M. Y. Chae, *J. Am. Chem. Soc.* **2007**, *129*, 9842.
[21] L. H. Xie, Q. D. Ling, X. Y. Hou, W. Huang, *J. Am. Chem. Soc.* **2008**, *130*, 2120.
[22] Y. Jung, S. H. Lee, A. T. Jennings, R. Agarwal, *Nano Lett.* **2008**, *8*, 2056.
[23] A. Bandyopadhyay, A. J. Pal, *Appl. Phys. Lett.* **2004**, *84*, 999.
[24] H. Li, Q. F. Xu, N. J. Li, R. Sun, J. F. Ge, J. M. Lu, H. W. Gu, F. Yan, *J. Am. Chem. Soc.* **2010**, *132*, 5542.
[25] Q. D. Ling, D. J. Liaw, E. Y. H. Teo, C. X. Zhu, D. S. H. Chan, E. T. Kang, K. G. Neoh, *Polymer* **2007**, *48*, 5182.
[26] H. Li, Z. N. Jin, N. J. Li, Q. F. Xu, H. W. Gu, J. M. Lu, X. W. Xia, L. H. Wang, *J. Mater. Chem.* **2011**, *21*, 5860.
[27] C. L. Liu, T. Kurosawa, A. D. Yu, T. Higashihara, M. Ueda, W. C. Chen, *J. Phys. Chem. C* **2011**, *115*, 5930.
[28] J. Lee, E. Lee, S. Kim, G. S. Bang, D. A. Shultz, R. D. Schmidt, M. D. E. Forbes, H. Lee, *Angew. Chem. Int. Ed. Engl.* **2011**, *50*, 4414.
[29] S. L. Lim, Q. D. Ling, E. Y. H. Teo, C. X. Zhu, D. S. H. Chan, E. T. Kang, K. G. Neoh, *Chem. Mater.* **2007**, *19*, 5148.
[30] G. Liu, B. Zhang, Y. Chen, C. X. Zhu, L. Zeng, D. S. H. Chan, K. G. Neoh, J. Chena, E.T. Kang, *J. Mater. Chem.* **2011**, *21*, 6027.
[31] Y. K. Fang, C. L. Liu, W. C. Chen, *J. Mater. Chem.* **2011**, *21*, 4778.
[32] X. D. Zhuang, Y. Chen, G. Liu, P. P. Li, C. X. Zhu, E. T. Kang, K. G. Neoh, B. Zhang, J. H. Zhu, Y. X. Li, *Adv. Mater.* **2010**, *22*, 1731.
[33] Q. D. Ling, Y. Song, S. J. Ding, C. X. Zhu, D. S. H. Chan, D. L. Kwong, E. T. Kang, K. G. Neoh, *Adv. Mater.* **2005**, *17*, 455.

[34] E. Y. H. Teo, Q. D. Ling, Y. Song, Y. P. Tan, W. Wang, E. T. Kang, D. S. H. Chan, C. X. Zhu, *Org. Electron.* **2006**, *7*, 173.
[35] W. Kwon, B. Ahn, D. M. Kim, Y. G. Ko, S. G. Hahm, Y. Kim, H. Kim, M. Ree, *J. Phys. Chem. C* **2011**, *115*, 19355.
[36] J. K. Choi, S. Jang, K. J. Kim, H. Sohn, H. D. Jeong, *J. Am. Chem. Soc.* **2011**, *133*, 7764.
[37] M. J. Frisch, G. W. Trucks, H. B. Schlegel, G. E. Scuseria, M. A. Robb, J. R. Cheeseman, J. A. Montgomery Jr., T. Vreven, K. N. Kudin, J. C. Burant, J. M. Millam, S. S. Iyengar, J. Tomasi, V. Barone, B. Mennucci, M. Cossi, G. Scalmani, N. Rega, G. A. Petersson, H. Nakatsuji, M. Hada, M. Ehara, K. Toyota, R. Fukuda, J. Hasegawa, M. Ishida, T. Nakajima, Y. Honda, O. Kitao, H. Nakai, M. Klene, X. Li, J. E. Knox, H. P. Hratchian, J. B. Cross, V. Bakken, C. Adamo, J. Jaramillo, R. Gomperts, R. E. Stratmann, O. Yazyev, A. J. Austin, R. Cammi, C. Pomelli, J. W. Ochterski, P. Y. Ayala, K. Morokuma, G. A. Voth, P. Salvador, J. J. Dannenberg, V. G. Zakrzewski, S. Dapprich, A. D. Daniels, M. C. Strain, O. Farkas, D. K. Malick, A. D. Rabuck, K. Raghavachari, J. B. Foresman, J. V. Ortiz, Q. Cui, A. G. Baboul, S. Clifford, J. Cioslowski, B. B. Stefanov, G. Liu, A. Liashenko, P. Piskorz, I. Komaromi, R. L. Martin, D. J. Fox, T. Keith, M. A. Al-Laham, C. Y. Peng, A. Nanayakkara, M. Challacombe, P. M. W. Gill, B. Johnson, W. Chen, M. W. Wong, C. Gonzalez, J. A. Pople, Gaussian 03, revision C.02; Gaussian, Inc.: Wallingford, CT, **2004**.